$ 600,00

FT72.15.J4

THERMOELECTRIC POWER OF SOME METALLIC GLASSES

by

Mario Norberto Baibich

Submitted in partial fulfilment
of the requirements for the degree of
Master of Science

Department of Physics
McGill University
Montreal, Canada

August 1979.

A B S T R A C T

The thermoelectric power of five amorphous metallic alloys have been measured between 4 and 300 K. The alloys studied are the commercially available Metglas alloys (specifically Metglas 2204, 2826, 2826A, 2605 and 2605A).

Of these , only the nonferromagnetic alloy (Metglas 2204), agrees with the predictions of the modified Ziman theory in the temperature range studied. The reduction of the Kondo-type contributions to the thermoelectric power due to the Nordheim-Görter rule made impossible the detection of these effects. The thermoelectric power of amorphous metals will only be sensitive to the predominant scattering. The introduction of Cr or Mo in the composition of the alloys induces a reduction in the magnitude of the thermoelectric power by a factor of about 2.

R E S U M E

Le pouvoir thermoélectrique de cinq alliages amorphes a été étudié entre 4 et 300K.

Les alliages étudiés sont les Metglas commercialement disponibles (précisément Metglas 2204, 2826, 2826A et 2605A). Parmi ceux-ci seulement l'alliage nonferromagnétique dans l'écart de température étudié (Metglas 2204) correspond aux prédictions de la théorie modifiée de Ziman. La réduction des contributions du type Kondo au pouvoir thermoélectrique, due à la règle de Nordheim-Gürter, n'a pas permis la détection de ces effets.

Le pouvoir thermoélectrique des métaux amorphes sera sensible seulement à la diffusion prédominante.

L'introduction de Cr ou Mo dans la composition de l'alliage apporte une réduction du pouvoir thermoélectrique par un facteur approximativement égal à 2.

ACKNOWLEDGEMENTS

The author wishes to thank his research director, Dr. W.B. Muir, for all his help and advice.

Thanks is also due to all the people from the fourth floor of the Rutherford Physics Building for all the moral support, technical help and the feeling of really belonging to a group received throughout this work.

Financial assistance in the form of a scholarship was received from CNPq (Brazil).

Finally, the author wishes to thank his wife, Ione, for giving him a son, Roberto, encouragement, support and the essence of life: love.

TABLE of CONTENTS

ABSTRACT	i
ACKNOWLEDGEMENTS	iii
LIST of FIGURES	v
LIST of TABLES	v
CHAPTER I - Introduction	1
CHAPTER II - Experimental	5
1 The Cryostat	5
2 Method	7
3 Samples	8
CHAPTER III- Theory	10
1 Thermoelectric Power	10
2 Thermoelectric Power of Amorphous Metals	14
CHAPTER IV - Results and Discussion	22
1 Experimental Results	22
2 Liquid Metal Model	28
3 Kondo or Pseudo-Kondo Models	29
4 Structure Correlation	33
5 Effect of the Composition of the Alloy	34
6 General Considerations	36
CHAPTER V - Conclusions	37
BIBLIOGRAPHY	39

LIST of FIGURES

		PAGE
Figure 1	The electrical resistivities of some metallic glasses	3
Figure 2	Schematic diagram of the cryostat	6
Figure 3	Typical experimental output as obtained from the X-Y Plotter	9
Figure 4	Schematic diagram showing the liquid structure factor, the pseudo potential and their product	16
Figure 5	Integrated thermoelectric power for Metglas 2204	25
Figure 6	Integrated thermoelectric power for Metglas 2826 and 2826A	26
Figure 7	Integrated thermoelectric power for Metglas 2605 and 2605A	27
Figure 8	Thermoelectric power for Metglas 2204	30
Figure 9	Thermoelectric power for Metglas 2826 and 2826A	31
Figure 10	Thermoelectric power for Metglas 2605 and 2605A	32
Figure 11	Thermoelectric power for Metglas 2204, 2826, 2826A, 2605 and 2605A	35

LIST of TABLES

Table I	Some relevant information about the Metglas alloys studied	23

I. INTRODUCTION

Amorphous materials have been extensively studied in the past few years. In particular, great interest has focused on metallic glasses.

Those materials, in common with their non metallic counterparts, possess no long range structural order although a certain degree of short range order is preserved. For metallic amorphous alloys this short range order is limited to a much smaller distance than that found for amorphous covalent semiconductors or insulators.[1]

The composition of metallic glasses can be classified into two groups:

(a) alloys of transition or noble metals with a metalloid of group IV or V acting as a glass former, e.g. $Fe_{80}B_{20}$

(b) alloys not containing glass formers, e.g. CuZr, MgZn, TbFe, etc.

The usual production techniques for metallic glasses include among others:

(a) deposition from a liquid solution

(b) rapid quenching from the melt

(c) evaporation

(d) sputtering

(e) chemical precipitation.

The magnetic properties of amorphous metals have been widely studied due to the potential commercial use of these materials as transformer cores, magnetic shielding and permanent magnets. The mechanical properties are also of interest as some of these materials possess tensile strength comparable to the strongest steels.[2]

In order to gain further fundamental understanding of the nature of these materials electron transport studies have been undertaken by various investigators.[3] In particular the conductivity of metallic glasses has been studied over four orders of magnitude on the temperature scale (~50 mK to ~700°C). The total change seen over this wide range of temperatures does not exceed, in general, 10 % of the total resistivity.

A typical value for the resistivity of amorphous metals would be in the 100 to 300μΩ-cm range. Fig. 1 shows some of the curves obtained experimentally for the resistivity of metallic glasses.

In most amorphous metals a region with negative temperature coefficient is present, whether followed by a minimum or not. Also, the functional form of the resistivity is not usually modified by the presence of a strong magnetic field (~50 kG) although its magnitude may change due to domain effects and the normal orbital magnetoresistance.

These last two characteristics prompted a controversy over which theory would best describe the transport phenomena

Figure 1. The Electrical Resistivities of Some Metallic Glasses

(a) the resistivities of some Metglas alloys and CoP, after R.W. Cochrane and J.O.Ström-Olsen, J. Phys. F7, no.9, 1799 (1977).

(b) the resistivities of two samples of Metglas 2605A,after R.W. Cochrane.[1]

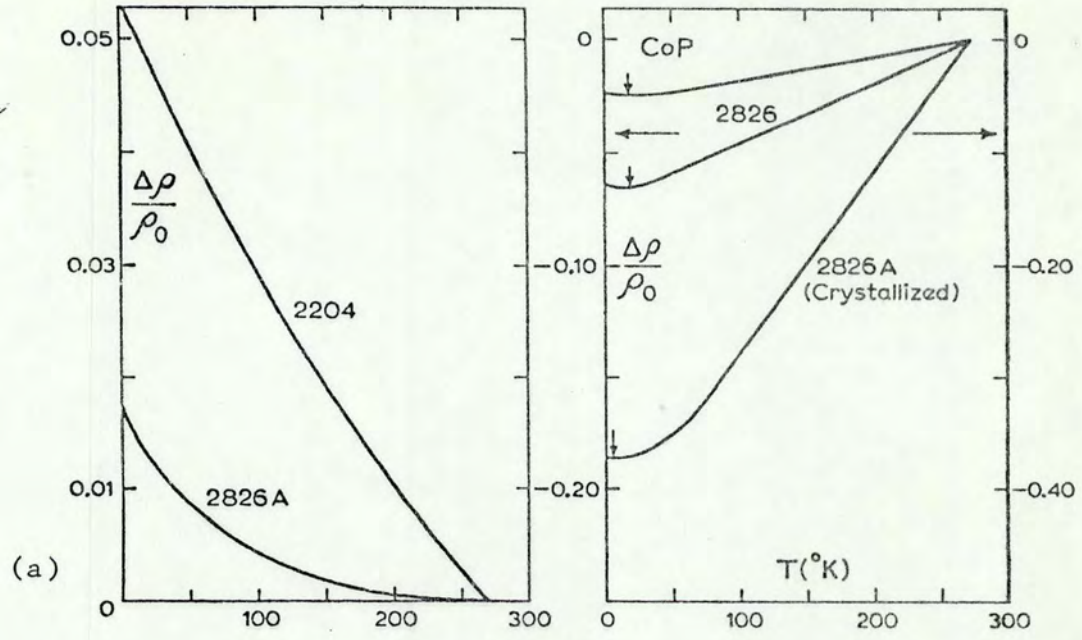
(a)
0.05
0.03
0.01
0
$\frac{\Delta\rho}{\rho_0}$
2204
2826A
100
200
300
CoP
2826
$\frac{\Delta\rho}{\rho_0}$
2826A
(Crystallized)
0
-0.10
-0.20
-0.40
T(°K)

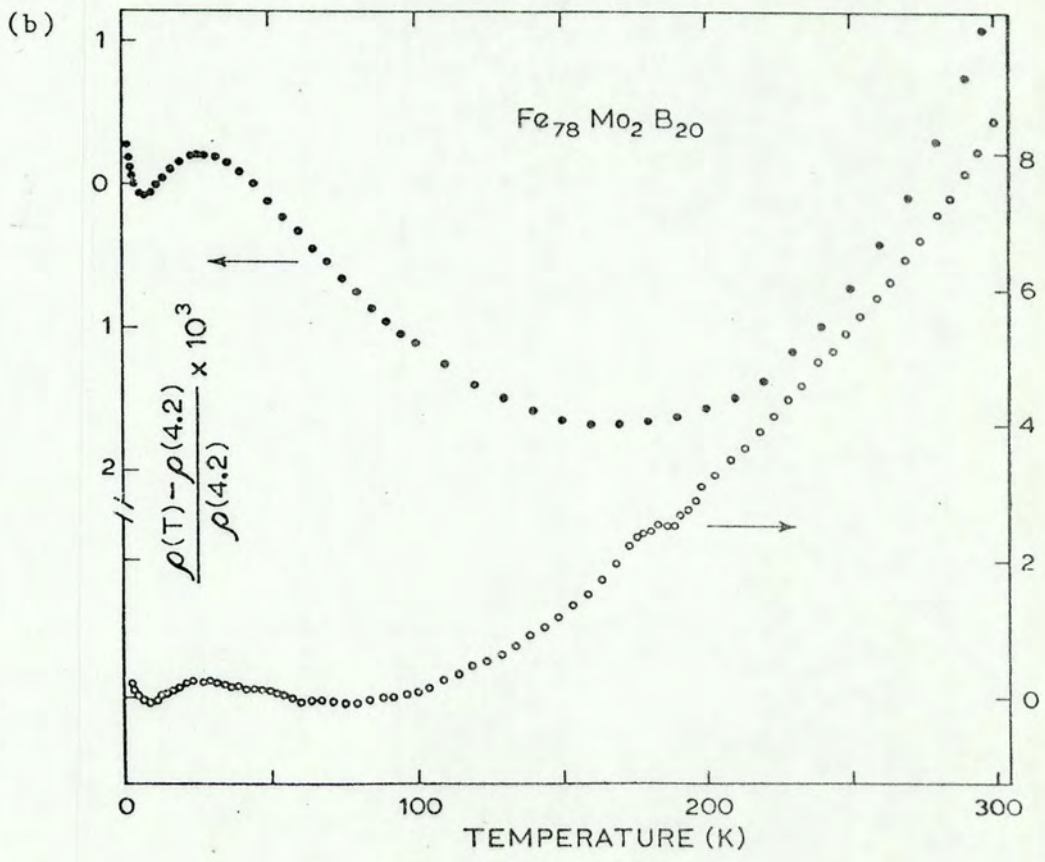
(b)
$Fe_{78}\ Mo_2\ B_{20}$
$\frac{\rho(T)-\rho(4.2)}{\rho(4.2)} \times 10^3$
1
0
1
2
8
6
4
2
0
100
200
300
TEMPERATURE (K)

in amorphous metals. The theories advanced to explain electron conduction in metallic glasses comprise 1) an extension of Ziman's liquid metal theory, 2) the Kondo effect where only some of the magnetic ions in the alloy contribute to the anomalous scattering and 3) a Kondo-type theory where structural degrees of freedom replace the degrees of freedom provided by the spin orientations in the normal Kondo effect.

The objective of this work is to compare the predictions of the existing theories with our experimental results for the thermoelectric power of amorphous metals.

We have measured the thermoelectric powers of a series of metallic glasses between 4K and 300K and we compare the results to the predictions of the extended Ziman theory and to the Kondo or Kondo-like theories advanced to explain the behaviour of the resistivity. We also discuss the effect of the presence of certain transition elements such as Cr and Mo on the thermoelectric power.

The study of the thermoelectric power was chosen as a technique because it is, for crystalline materials, generally a more sensitive probe of the scattering processes than is the electrical resistivity. Also, at the start of this work no measurements of the thermoelectric power of amorphous metals had been published ; however, just before this work was completed results on Metglas 2204 were published by Nagel.[4]

II. EXPERIMENTAL

II. 1 - The Cryostat

The cryostat used for these experiments is shown schematically in Fig. 2. It consists basically of two copper clamps mounted on a phenolic tube to hold the sample. The top clamp has a heater mounted on the back of the copper block, as well as a calibrated Si diode to measure the temperature. The 110 Ω heater, made of 38 BS CuNi wire, is non inductively wrapped around the block and held in good thermal contact with it by means of GE 7031 varnish. This heater is driven by a DC current source up to 300 mA.

The sample is located between the two clamps, and is connected to a reversing switch located below the bottom clamp. The connection from the bottom block to the reversing switch is made through copper wire. The top clamp is connected to the reversing switch through a thick wire made of 5N pure Pb which is clamped to the block together with the sample.

The leads connecting the switch, heater and thermometer to the terminal board at the top of the cryostat are twisted pairs of # 40 BS FORMEL covered copper wire, thermally anchored to the phenolic tube with GE 7031 varnish wherever possible.

The reversing switch was made from a ceramic 8 pole 3 position switch, manually operated from the top of the cryostat.

Figure 2 Schematic diagram of the cryostat

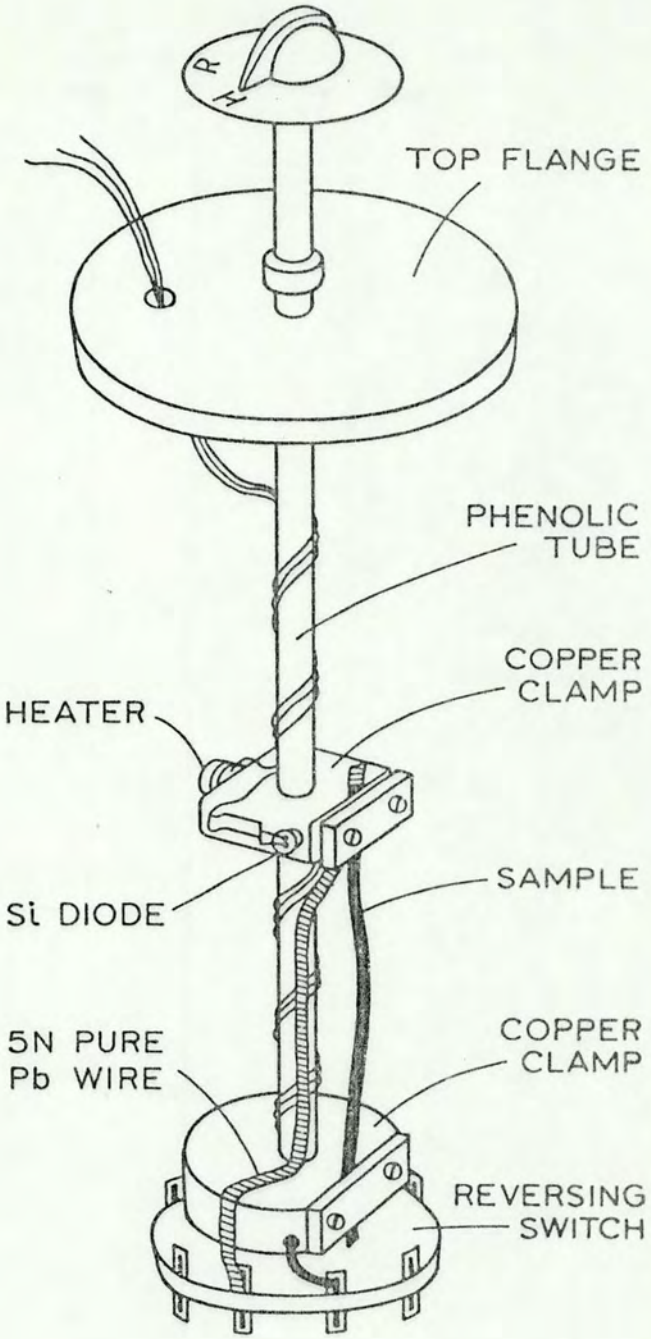
R
H
TOP FLANGE
PHENOLIC TUBE
COPPER CLAMP
HEATER
SAMPLE
Si DIODE
5N PURE Pb WIRE
COPPER CLAMP
REVERSING SWITCH

The thermoelectric power apparatus is placed inside a double dewar assembly which allows either liquid nitrogen or liquid helium to be used as refrigerant.

II-2 - METHOD

The experiments were performed by first immersing both clamps in the refrigerant and then lifting the top clamp from the bath in order to vary its temperature. The bottom clamp and reversing switch were kept in the bath at all times during the experiment.

By varying the current flowing through the heater, the temperature of the top clamp was controlled. This temperature was monitored through a 4 terminal DC measurement of the forward resistance of a Si diode. The DC current source for the thermometer was maintained at 10 μA through the whole range of temperatures and the voltage was read on a digital voltmeter whose analog output was connected to the x-axis of an XY recorder.

The experiments proceeded by sweeping the temperature while reversing the switch periodically. The voltage generated by the temperature gradient on the lead-sample thermocouple was measured by a Keithley Model 148 Nanovoltmeter whose analog output was connected to the y-axis of the XY recorder previously referred to. Both heating and cooling curves were plotted so that correction could be made for any temperature gradient in the top copper block.

The use of the reversing switch with each measurement

eliminates stray thermal EMF's and effects of equipment drifts. A typical example of the experimental output can be seen in Fig. 3.

II - 3 - Samples

These experiments were performed on amorphous metals with compositions listed below. They were obtained from Allied Chemical Company as thin ribbons and were produced by rapid quenching from the melt.

The samples were cut to size and installed in the cryostat without any heat treatment to avoid crystallization.

The alloys used in these experiments were:

BRAND NAME[5]	COMPOSITION
Metglas 2826	$Fe_{40}Ni_{40}P_{14}B_6$
Metglas 2826A	$Fe_{32}Ni_{36}Cr_{14}P_{12}B_6$
Metglas 2605	$Fe_{80}B_{20}$
Metglas 2605A	$Fe_{78}Mo_2B_{20}$
Metglas 2204	$Ti_{50}Zr_{10}Be_{40}$

Figure 3 Typical experimental output as obtained from the X-Y Plotter.
The horizontal axis corresponds to the reading of the Si diode used as a thermometer. The vertical axis is obtained from the output of the nanovoltmeter used to measure the voltage generated by the pair sample - lead.

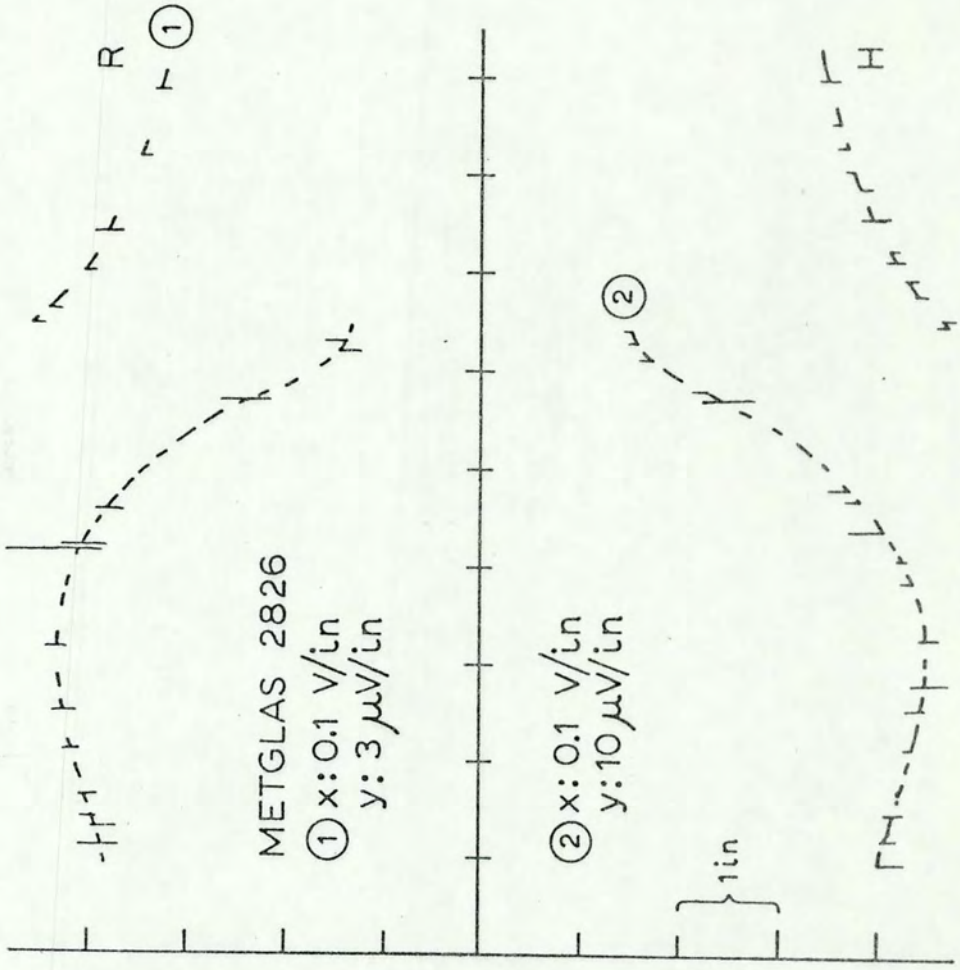
METGLAS 2826
① x: 0.1 V/in
y: 3 μV/in
② x: 0.1 V/in
y: 10 μV/in
1in

III - THEORY

III-1 - Thermoelectric Power

The electron transport properties of a metal can be investigated using Boltzmann's equation for electronic processes within the metal. Boltzmann's equation can be formally written as:

$$\left(\frac{df}{dt}\right)_{fields} + \left(\frac{df}{dt}\right)_{collisions} = 0$$

where f stands for the electron distribution function in the metal.

The fields that we are referring to in the steady state equation above are electric or magnetic fields and temperature gradients. The effect of those fields on the electron gas will be compensated by collisions.

Assuming that the collision term will be a simple exponential function, in other words, that the steady state will be restored by an exponential decay from higher energy states, we can define a relaxation time "τ" and solve the Boltzmann equation. With this approximation, we can study transport phenomena by applying electric or magnetic fields or temperature gradients, or any combination of those to a system of electrons and analyzing the behaviour of τ.

If we apply an electric field only, we get a quantity called electrical conductivity (σ), which relates the electric field applied to the electric current density generated.

By applying a thermal gradient only , we can study the thermal conductivity (κ), that relates the heat flow to the thermal gradient to the sample. Since the carriers of heat in this situation are mainly electrons, an electric current will be present and thus a voltage will develop between the ends of the sample. This difference of potential between the two points at different temperatures will be related to both the thermal gradient applied and the conductivity of the sample. This effect, called THERMOELECTRIC POWER or SEEBECK EFFECT, relates the thermal gradient applied to the consequent electric field.

Schematically, we can represent the situation like this:

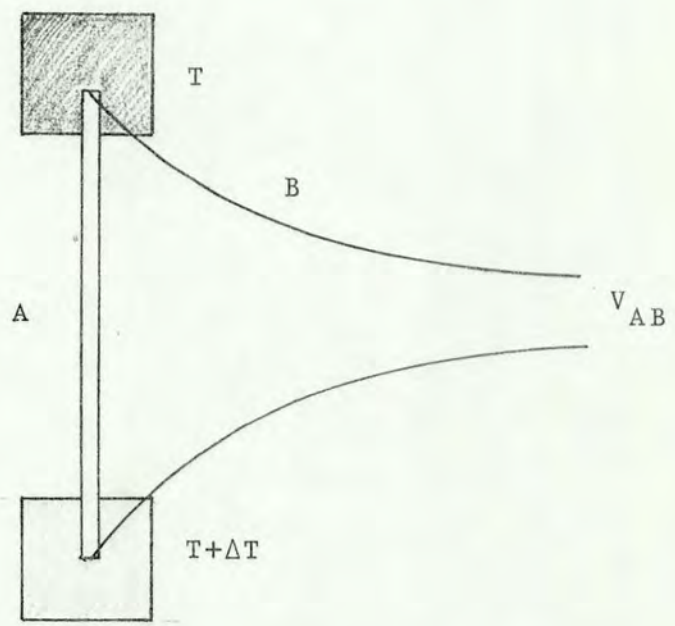

If $\Delta T/_T$ <<1, we can define the relative thermoelectric

power S_{AB} as

$$S_{AB} = \frac{\Delta V_{AB}}{\Delta T}$$

It is clear from the figure above that we need two different metals to measure ΔV_{AB}, implying that we only know from the experiment the relative thermoelectric power. Defining the absolute thermoelectric power S_A and S_B by

$$S_{AB} = S_A - S_B$$

and knowing the absolute thermoelectric power for one metal we can obtain the absolute thermoelectric power for any other metal.

The thermoelectric power for a superconductor is zero due to the condensation of the electrons in the superconducting state. In other words, the electrons in a superconductor are all used for electrical conduction turning the materials into a perfect heat insulator below its transition temperature. Thus, if one measures the Seebeck voltage of a pair formed by a superconductor and another metal one obtains directly the absolute thermopower for that metal. This method is used for low temperature measurements of thermoelectric power. For temperatures above the range of superconducting transition temperatures a known standard for thermoelectric power should be used as the other arm of the thermocouple.

The absolute thermoelectric power of the standard can be determined by measuring the Thomson coefficient for the

material and then using the Kelvin relation to find the absolute thermoelectric power.

The Thomson coefficient μ_T is defined by:

$$\dot{Q} = \rho J^2 - \mu_T J \nabla T$$

where $\dot{Q}$ is the rate of heat production in a current carrying sample, ρ is its resistivity, J is the current density and ∇T the temperature gradient.

Experimentally one establishes a known temperature gradient and forces a known current through the sample, measuring the amount of heat absorbed or released in the process. This effect is related to the thermoelectric power through the Kelvin relation:

$$S = \int_0^T \frac{\mu_T}{T} \, dT$$

This method was used by Borelius[6] in 1928-32 and more recently by Roberts[7] to establish a widely accepted standard for the thermoelectric power of lead. Lead has the advantage of being a superconductor below 7.25K and having a relatively small thermoelectric power above that transition temperature.

A full discussion of thermoelectric effects in crystalline metals is given in MacDonald[8], Barnard[9] and in Blatt et al.[10]

III - 2 - Thermoelectric power for amorphous metals

The most characteristic feature of electron transport in amorphous metals is the existence of a region in temperature where the resistivity has a negative temperature coefficient. In some cases this region of negative temperature coefficient is followed by one of positive temperature coefficient resulting in a minimum in the resistivity.

Two groups of models have been proposed to explain the observed negative temperature coefficient of the resistivity. One group is based on extensions of the Kondo theory of the resistivity of dilute magnetic impurities in metals, while the other group is based on extensions of Ziman's theory of electron transport in liquid metals.

The first group of theories is only applicable at temperatures less than roughly 20 K while the second group of theories is applicable at higher temperatures.

Ziman's liquid metal model has recently been used by Nagel[4] in the interpretation of the thermoelectric power of a single amorphous alloy. The idea is that the amorphous metal is merely a frozen liquid and therefore all the expressions derived for the liquid are valid for the metallic glass.

Upon freezing of the liquid a relaxation time arises from the absence of translational symmetry in the ionic potential which produces incoherent electron scattering. This relaxation time, τ_z, is the only source of scattering considered in Ziman's theory of the resistivity of liquid metals

The relaxation time can be written in terms of the ionic pseudo-potential and the liquid structure factor. The ionic pseudo-potential is derived from the potentials associated with individual ions. The liquid structure factor may be inferred from X-ray and neutron diffraction experiments and it describes the scattering of electrons by the ion cores. For a totally random distribution of the ions, the structure factor would have a value of 1. Both the ionic pseudo-potential ($\mathcal{V}(\bar{K})$) and the liquid structure factor ($a(\bar{K})$), along with the product $a(\bar{K})|\mathcal{V}(\bar{K})|^2$, are shown schematically in Fig. 4.

The resistivity for liquids according to Ziman's theory can be written as:

$$\rho_z = \text{const} \quad \langle |\mathcal{V}(\bar{K})|^2 \, a(\bar{K}) \rangle$$

where $$\langle |\mathcal{V}(\bar{K})|^2 a(\bar{K}) \rangle \equiv \int_0^1 |\mathcal{V}(\bar{K})|^2 a(K) \quad 4\left(\frac{\bar{K}}{2k_F}\right)^3 \, d\left(2\frac{\bar{K}}{k_F}\right) ,$$

k_F is the Fermi wave vector and $\bar{K}$ is the momentum transfer in the process. The value $2k_F$ corresponds to the maximum possible momentum transfer. If $2k_F \simeq k_p$, where k_p is the position of the first peak in the structure factor, it can be seen from Fig. 4 that the resistivity will decrease with increasing temperature, since the peak in $a(\bar{K})$ will broaden and decrease its maximum value as the temperature rises.

From the expression for the resistivity it is possible to obtain an expression for the diffusion thermoelectric power

Figure 4 Schematic Diagram showing the Variation of

(a) the liquid structure factor ($a(\overline{K})$; $a(\overline{K}) \equiv 1$ corresponds to a completely random array)

(b) the ionic pseudo potential ($\mathcal{V}(\overline{K})$) and

(c) the product $a(\overline{K})\,|\mathcal{V}(\overline{K})|^2$ as functions of $\overline{K}$, after R.D. Barnard.[9]

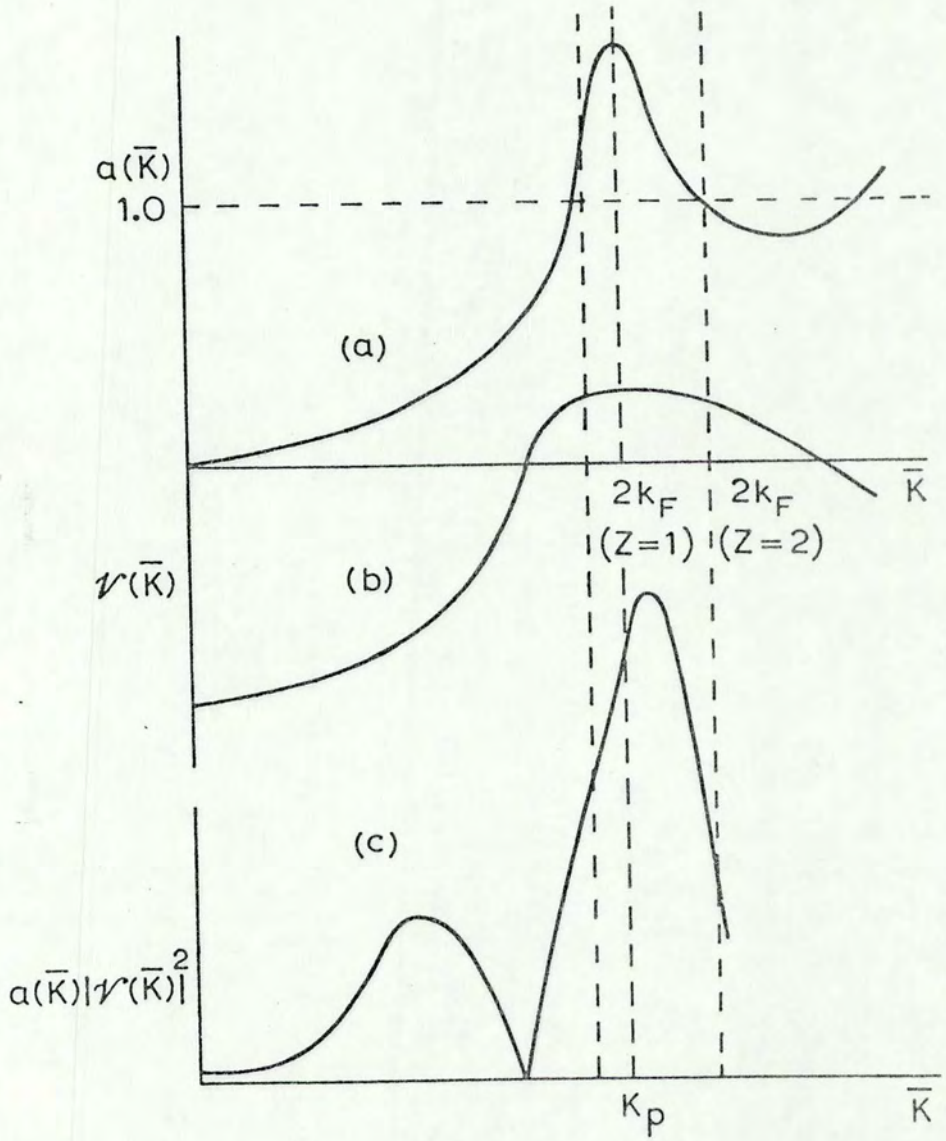
a(K̄)
1.0
(a)
2k_F
2k_F
K̄
(Z=1)
(Z=2)
𝒱(K̄)
(b)
(c)
a(K̄)|𝒱(K̄)|²
K_p
K̄

using $S \alpha \frac{1}{\rho} \left(\frac{\partial \rho}{\partial E} \right)_{E_F}$. This yields[9]

$$S_D = - \frac{\pi^2 k^2 T}{3|e|E_F} \xi$$

where $\xi = 3 - 2 \dfrac{|\mathcal{V}(2k_F)|^2 a(2k_F)}{\langle |\mathcal{V}(\bar{K})|^2 a(\bar{K}) \rangle} - \frac{1}{2} \dfrac{\left\langle k_F \dfrac{\partial |\mathcal{V}(\bar{K})|^2}{\partial k_F} a(\bar{K}) \right\rangle}{\langle |\mathcal{V}(\bar{K})|^2 a(\bar{K}) \rangle}$

or $\xi = 3 - 2q - \frac{1}{2} r$

Although in most cases r turns out to be small, this term is necessary because the pseudo-potential is energy dependent as well as K dependent.

In this theory, the thermoelectric power should be a linear function of temperature with the sign dependent on the magnitude of q and r.

As can be seen from Fig. (4), if $2k_F \simeq k_p$ the parameter q will dominate and, for most cases, a positive thermoelectric power would be expected when electrons are the charge carriers.

The claim made by Nagel[4] to explain his results for Metglas 2204 was that $2k_F \simeq k_p$. With this both the observed negative temperature coefficient of the resistivity and the positive thermoelectric power are obtained. The condition $2k_F \simeq k_p$ was also indicated in a previous work by Nagel and Tauc[11] as a condition to obtain a stable amorphous alloy containing transition metals.

The other group of theories suggested to explain the behaviour of amorphous metals is based on Kondo's theory of the resistance minimum. This effect is found in crystalline alloys of non magnetic hosts with small concentrations of magnetic impurities. In Kondo's theory the extra scattering needed to form the minimum in ρ at low temperatures arises from transitions between the spin states of the magnetic ion.

Tsuei and Hasegawa [12] first proposed a Kondo mechanism to explain the results obtained for the resistivity of amorphous metallic alloys. Their claim was that some of the magnetic atoms would be in a negligibly small internal field, giving rise to a Kondo effect even when the sample was a ferromagnet.

Further studies of resistivity and magnetoresistance by Cochrane et al.[13] showed that the shape of the resistivity versus temperature curves is practically unchanged upon the application of fairly high magnetic fields (~50kG) in contrast to the results in crystalline Kondo alloys where the minimum is suppressed.[14] This led to the suggestion that the negative temperature coefficient of the resistivity is not due to magnetic interactions and that a common property of all amorphous metals should be used to explain the effect. Such common property is obviously the lack of crystalline structure.

Cochrane et al.[13] showed that the anomaly in the

resistivity could be caused by electrons scattering from structural degrees of freedom inherent in the lack of atomic periodicity in the material. In this model an ion is considered to be able to occupy either of two equivalent sites. The two tunneling levels can provide the necessary degrees of freedom which were provided by the spin orientations in the original Kondo effect.

This model runs into difficulty because at least one amorphous metal[15] is known to have its resistivity devoid of the characteristic minimum. If the minimum is due solely to structure, one would expect all amorphous metals to have it.

Recently Grest and Nagel[16] have modified Tsuei's original idea by including a distribution of internal fields that provides for the existence of Kondo effect in ferromagnets as well as for the insensivity to magnetic fields of the order of magnitude used by Cochrane et al.[13]

Grest and Nagel performed a Monte Carlo calculation of the effective fields that are present at each ion in a strong amorphous ferromagnet using measured radial distribution functions. Upon inclusion of super-exchange interactions between next nearest neighbor magnetic atoms separated by a metalloid atom, a long tail in the distribution of internal fields was obtained. This tail goes through zero and has a finite value at negative fields.

With these results they concluded that ferromagnetism

and Kondo effect could coexist in ferromagnetic metallic glasses and show no magnetic field dependence of the anomalous part of the resistivity. This is due to the presence of a small concentration of magnetic atoms which are located in nearly zero effective field at all applied external magnetic fields, thus repeating the conditions for the original Kondo effect.

For all Kondo or Kondo-like theories, one can write the anomalous resistivity as

$$\rho = \rho_o - C \ln(T^2+\Delta^2)$$

where C and Δ have different physical origins according to each of the theories. ρ_o represents all temperature independent scattering.

In the case of the distribution of effective fields, C represents a constant proportional to the concentration of magnetic impurities located in zero field and Δ represents the energy splitting between the two spin states.

In the tunneling theory, C represents both the Coulomb interaction between the ion and the electron and the concentration of tunneling states and Δ is the characteristic energy splitting for the levels of the double well potential of the tunneling state.

Since the Hamiltonians describing both the Kondo-like problems are identical to the original Kondo Hamiltonian, we expect all these models to have similar results for the thermoelectric power.

The Kondo theory of dilute magnetic alloys accounts for the "giant thermoelectric power" observed in these alloys. This thermoelectric power can be as big as 16 μV/K at 10K or about an order of magnitude larger than the normal diffusion thermoelectric power.

Although no extensions of any of the modified Kondo theories to thermoelectric power of amorphous metals are known, the thermoelectric power can be expected to behave in much the same way as that observed in the original Kondo systems, that is, presenting extrema in the thermoelectric power around the equivalent of the Kondo temperature.

IV RESULTS AND DISCUSSION

IV - 1 - Experimental Results

We have measured the thermoelectric powers of a series of metallic glasses between 4K and 300K using the cryostat and method described in Chapter II.

The experimental results obtained for the different samples were analyzed by first substracting the values for the integrated thermoelectric power of Pb as published by Roberts.[7] With this, a plot of the integrated thermoelectric power of the sample can be drawn (Figs. 5,6,7). The data is then differentiated graphically and the results are shown in Figs. 8,9,10.* The error, estimated to be about 3 %, comes mainly from the chosen graphical differentiation method and is evident when analyzing the scatter of the experimental points obtained. The error implied in the measurement of the sample-lead pair voltages is determined by the accuracy of the instruments used, typically within 1 %. This was verified by measuring voltages generated at constant temperature by means of injecting a known D.C. current through a known resistance. All the experimental results are summarized in Fig. 11.

Table I shows the alloys measured and relevant information such as the composition, the temperature for the minimum in resistivity, the slope of the resistivity, the Curie temperature and the resistivity at room temperature.

---

*These results are presented along with those found by Elzinga and Schroeder (MSU) and Bélanger and Destry (U of M.). The results were submitted to publication in Phys. Lett. by all six authors (Baibich, Muir, Bélanger, Destry, Elzinga, Schroeder

TABLE I

METGLAS ALLOY	COMPOSITION	ρ_{273} ($\mu\Omega$cm)	$\frac{1}{\rho}\frac{d\rho}{dt}$ at 200K	T_{min} (K)	FERROMAGNETIC T_c (K)
2204	$Ti_{50}Be_{40}Zr_{10}$	300	-2×10^{-4}	300	non magnetic
2826	$Fe_{40}Ni_{40}P_{14}B_6$	180	$+2.3\times10^{-4}$	20	>300
2826A	$Fe_{32}Ni_{36}Cr_{14}P_{12}B_6$	180	-2.5×10^{-5}	270	249
2605	$Fe_{80}B_{20}$	140	$+1.0\times10^{-4}$	70	375
2605A	$Fe_{78}Mo_2B_{20}$	120	$+1.0\times10^{-4}$	10 & 70	>300

Our data for Metglas 2204 (Fig. 8) agrees extremely well with that of Nagel, and is linear in temperature above 40K. This straight line does not intercept the origin and therefore some change in slope should be expected as the temperature decreases. In the inset of Fig. 8 it can be seen that the thermoelectric power is linear below 15K, and it seems to approach zero with that slope, at least down to 0.3K. (The data below 4K was collected in another independent experiment with a ^{3}He cryostat[17]). Between 15K and 40K some curvature is seen in S(T).

In Fig. 9 we show the results for Metglas 2605 and 2605A.

The thermoelectric power of Metglas 2605 is clearly not linear, showing a minimum around 234K, is negative in the entire region studied and it contains no "structure" to speak of.* Metglas 2605A is nearly linear, always negative in this temperature range, basically structureless, and shows a relatively small inflexion at around 160K.

Fig. 10 shows the thermoelectric power for Metglas 2826. The main features are a change in sign around 25K and a minimum around 250K. No structure was detected, but the fact that S is still rising as the temperature decreases indicates that at least one maximum at T <5K must occur in order to fulfil the thermodynamic condition that $S(T=0) \equiv 0$.

Fig. 10 also shows the thermoelectric power for Metglas 2826A. Here, again, a change in sign takes place around 123K and a minimum appears at about 70K.

---

* We believe that the structure seen in our data around 30K is a consequence of a corrugation or expansion in the temperature scale possibly due to oscillations in the diode voltage on a scale smaller than the grid used to calibrate the diode. This can be verified by analyzing the corresponding region for the total voltage measured in the experiment (Figs. 5,6,7).

Figure 5 Integrated thermoelectric power for Metglas 2204

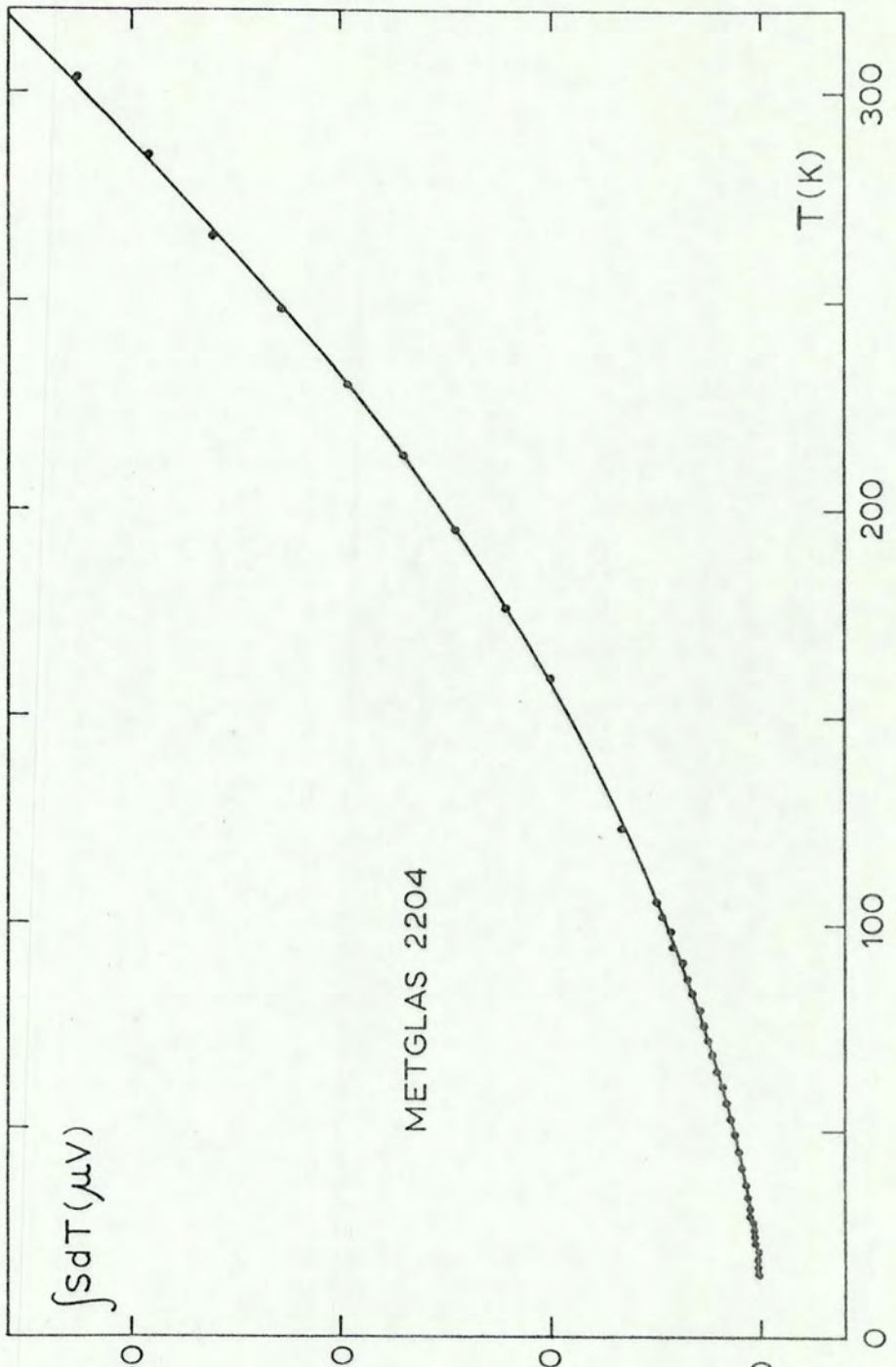
∫SdT (μV)
300
200
100
0
METGLAS 2204
0
100
200
300
T(K)

Figure 6 Integrated thermoelectric power for Metglas 2826 and 2826A

INSTITUTO DE FÍSICA

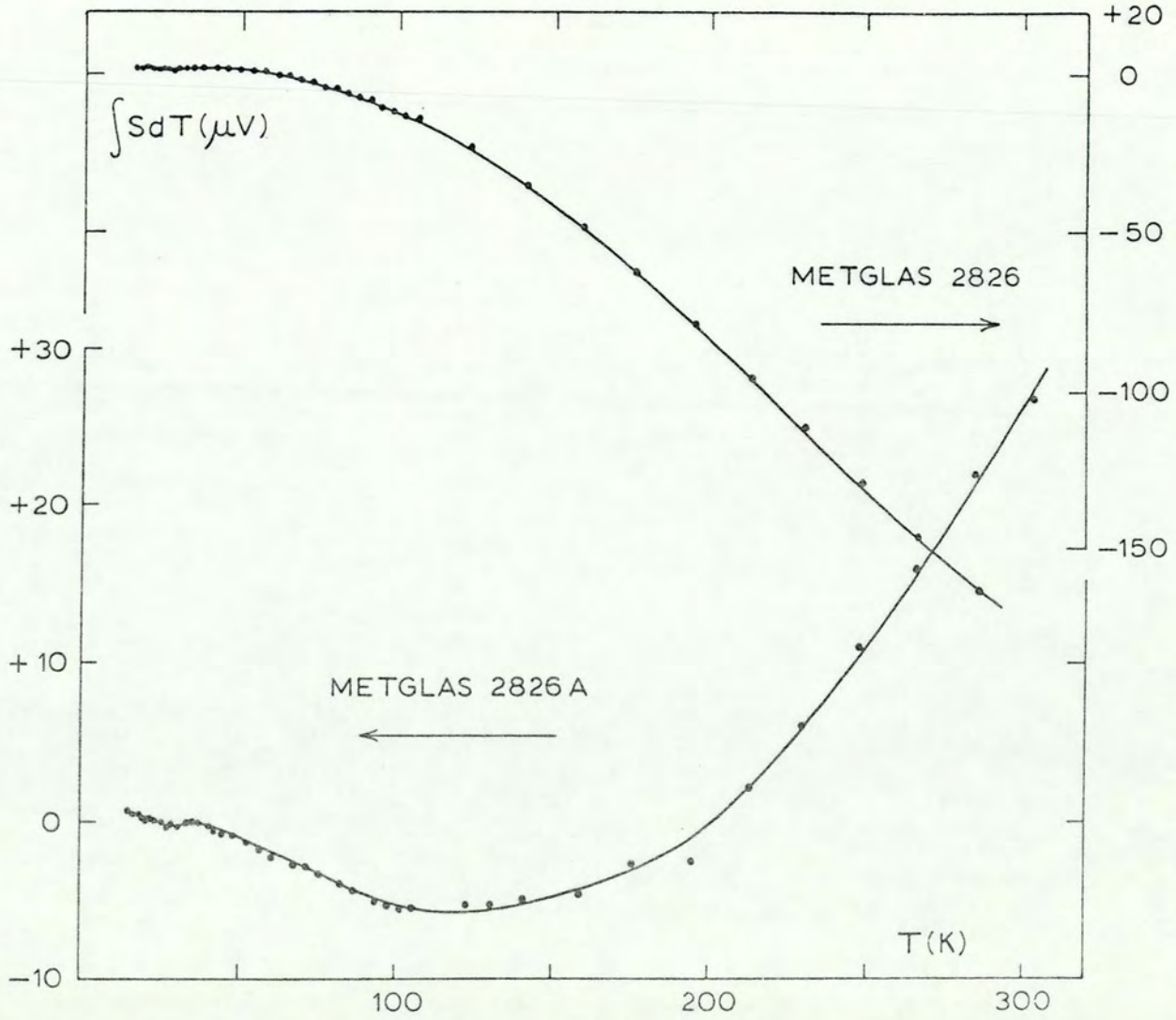
∫SdT(μV)
METGLAS 2826
METGLAS 2826 A
T(K)
+20
0
−50
−100
−150
+30
+20
+10
0
−10
100
200
300

Figure 7 Integrated thermoelectric power for Metglas 2605 and 2605A

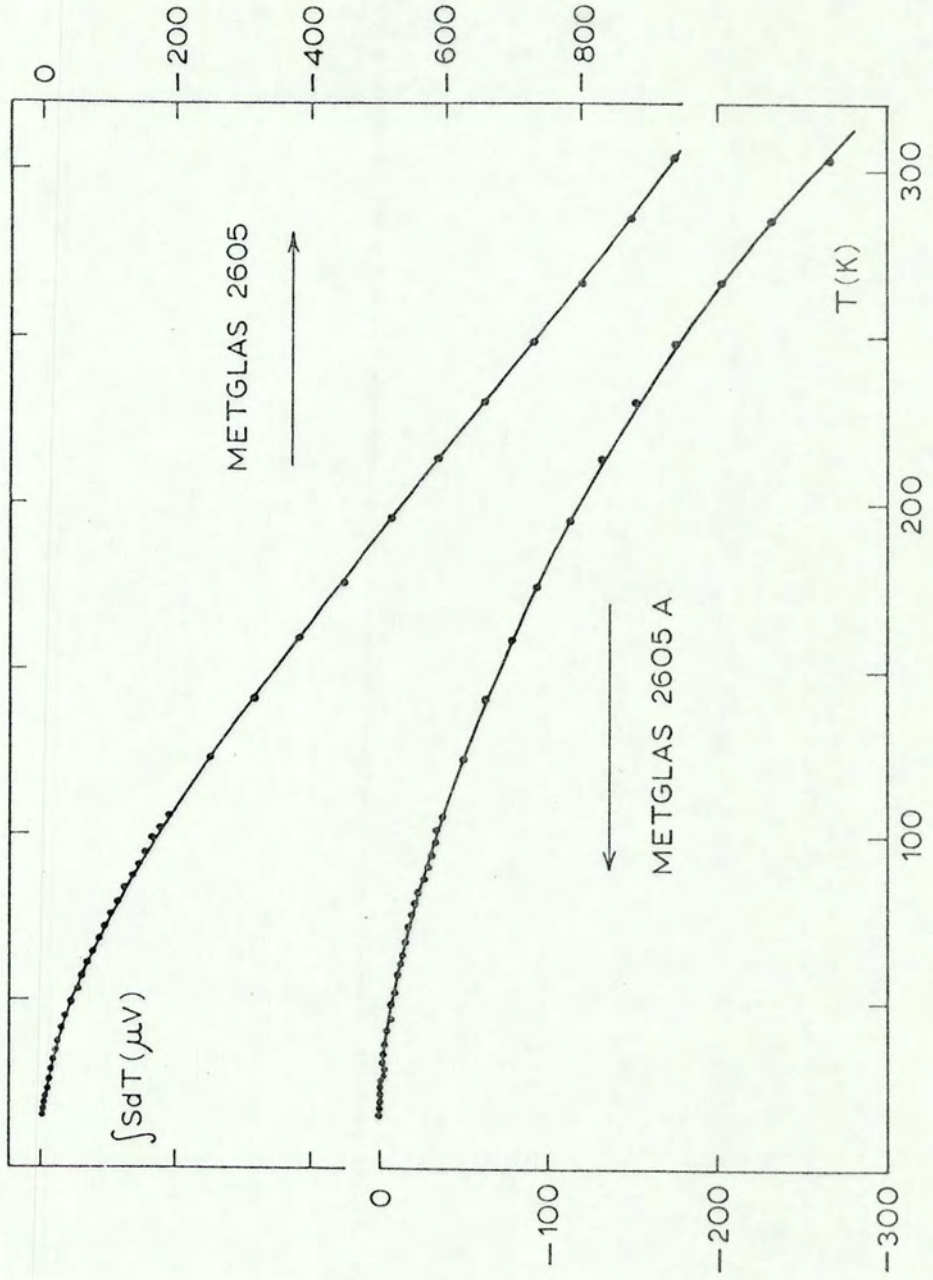
0
-200
-400
-600
-800
∫SdT (μV)
METGLAS 2605
METGLAS 2605 A
0
-100
-200
-300
100
200
300
T(K)

IV - 2 - Liquid Metal Model

The Ziman theory for transport phenomena in liquid metals is best applied to amorphous metals whose characteristic temperature for the minimum in resistivity is relatively high. In our case the samples fulfilling this requirement are Metglas 2204, 2826A and perhaps 2605 (see Table I).

As we discussed earlier, Metglas 2826A changes sign for the thermoelectric power at around 123K and shows a minimum at about 70K; Metglas 2605 is not linear and shows a minimum of the thermoelectric power at around 234K.

It then becomes clear that Metglas 2204 is the only sample from this group to have its thermoelectric power in good agreement with the predictions of a linear thermoelectric power for amorphous metals, as required in the modified Ziman theory.*

The fact that below 40K the thermoelectric power of Metglas 2204 does not follow the straight line predicted by the Ziman theory is not surprising since this theory becomes of doubtful value below 50K. The reason for this is that it does not include, in this first approximation, the inelastic nature of electron transitions arising out of ionic motion.(9)

*We should point out that Metglas 2204 is the only non ferromagnetic material in this group of alloys. However Metglas 2826A has its Curie temperature at 249K and there is no change in thermoelectric power in this temperature range thus indicating that the effect of ferromagnetism on the thermoelectric power is small.

On the other hand if we reverse the logic and say that a linear thermoelectric power would imply in a high T_{min}, then we would have to predict a high temperature minimum for the resistivity of Metglas 2605A. According to Rayne and Levy[18] this alloy shows a double minimum in resistivity, both minima below 70K.

IV-3 - Kondo or Pseudo-Kondo Models

All Kondo or Kondo-like models are valid for low temperatures, thus suggesting that the best results will be obtained for alloys with low T_{min}. In our case this means that we should include the alloys Metglas 2826 and perhaps 2605, 2605A.

The Kondo theories predict low temperature structure in the thermoelectric power. As it is seen from the experimetnal data, only Metglas 2826 might show a maximum of about 0.1μV/K. However, this apparent lack of structure in the Metglas thermoelectric power does not rule out the possibility of Kondo-like processes in these materials because of the consequences of the Nordheim-Gürter rule: The total thermoelectric power S can be written approximately in terms of the characteristic thermoelectric power S_i associated with the i^{th} scattering mechanism as[8]

$$S = \sum_i \frac{\rho_i}{\rho_T} S_i$$

Figure 8 Thermoelectric Power for Metglas 2204
The data obtained in this work is represented by solid dots. The solid triangles are the results obtained by Elzinga and Schroeder. The insert shows the results obtained in another independent experiment with a ^{3}He cryostat.[17]

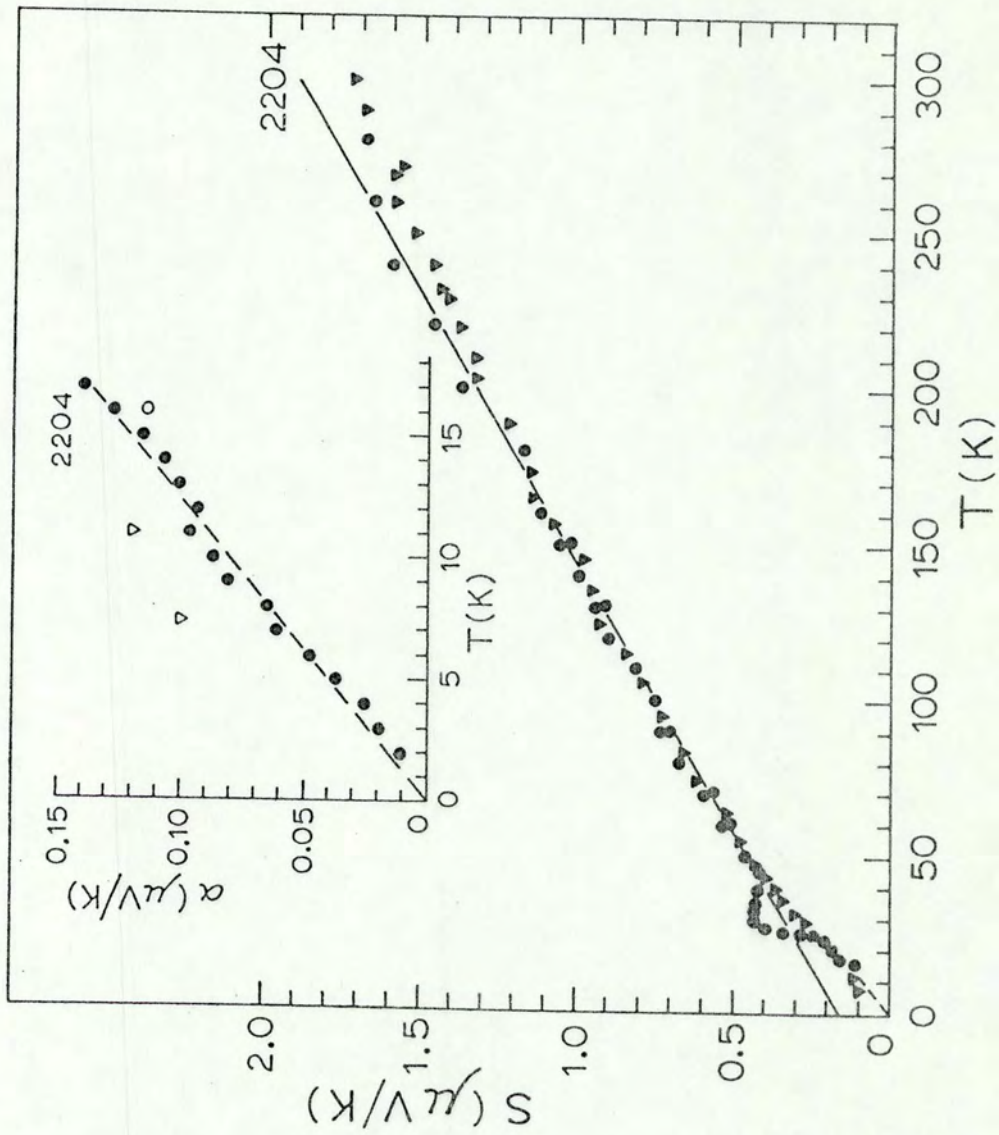
S (μV/K)
T (K)
2204
α (μV/K)
T(K)
2204

Figure 9

The following convention was used:

● - data obtained in this work

▲ - data obtained by Bélanger and Destry (Université de Montréal)

▼ - data obtained by Elzinga and Schröeder (Michigan State University)

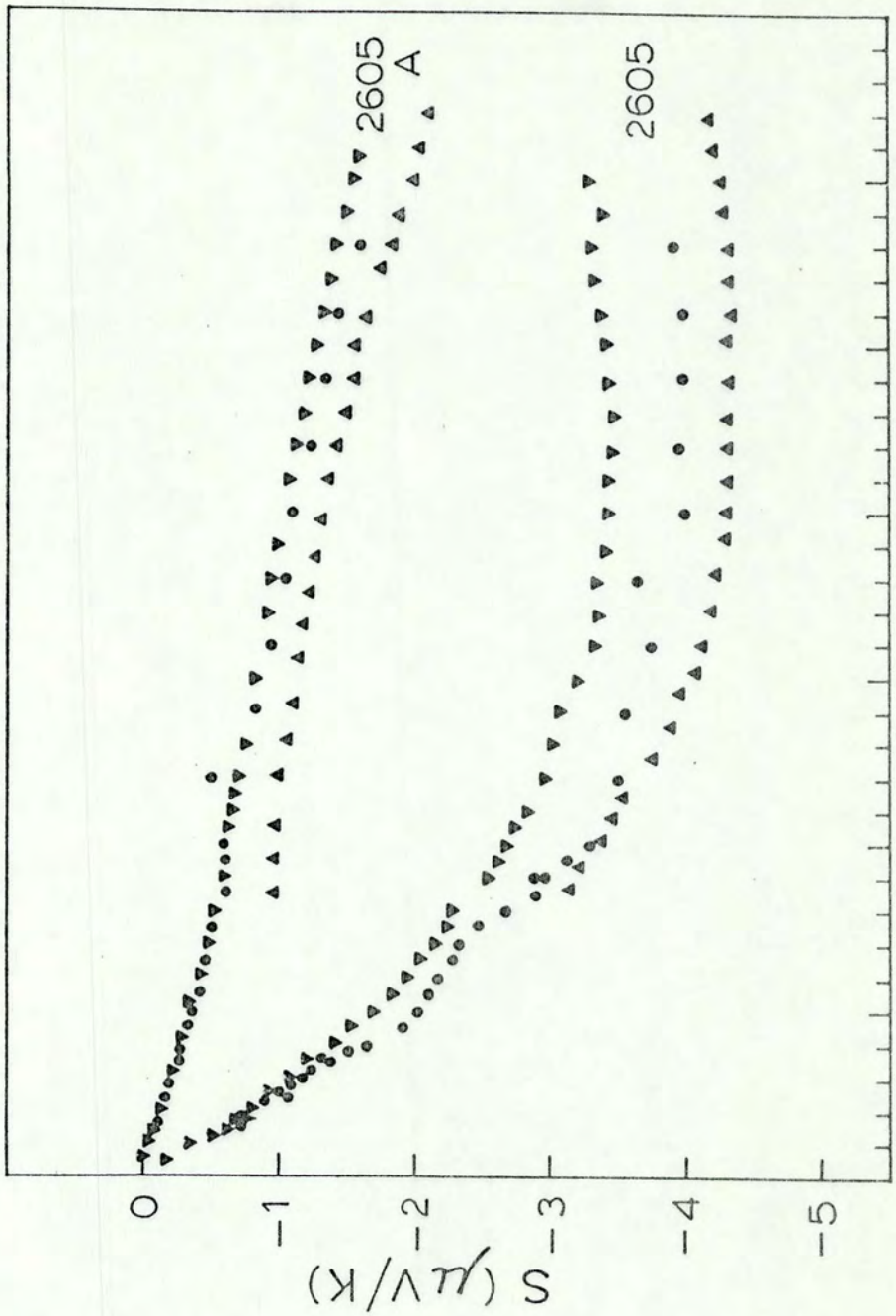
2605 A
2605
0
-1
-2
-3
-4
-5
S (μV/K)
0
100
200
300
T(K)

Figure 10

The following convention was used:

● - data obtained in this work

▲ - data obtained by Bélanger and Destry (Université de Montréal)

▼ - data obtained by Elzinga and Schröeder (Michigan State University)

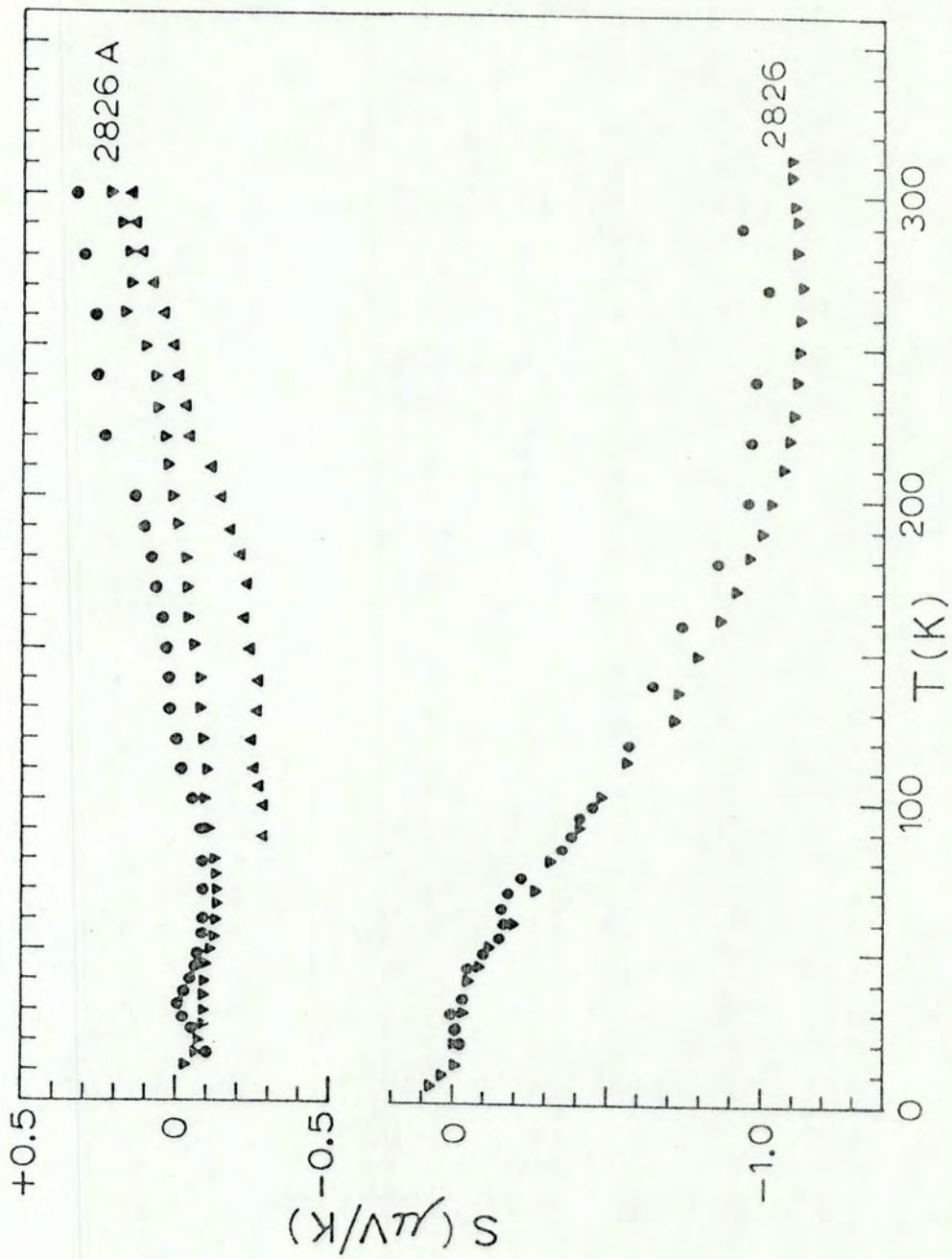
2826 A
2826
+0.5
0
-0.5
0
-1.0
0
100
200
300
T(K)
S (μV/K)

where ρ_i is the resistivity associated with the i^{th} scattering mechanism and ρ_T is the total resistivity. In particular

$$S = \frac{\rho_K}{\rho_T} S_K + \frac{\rho_o}{\rho_T} S_o$$

where the K^{th} mechanism is the Kondo or pseudo-Kondo contribution and the o^{th} is an approximation to all other effects. From the resistivity results $\frac{\rho_K}{\rho_T} \sim 10^{-3}$ so that $S \sim 10^{-3} S_K + S_o$.

The main result of this is that our resolution of about 0.1μV/K represents a Kondo-type contribution of about 100μV/K, which is at least twice as large as the highest peak known for thermoelectric power on crystalline Kondo systems.

IV - 4 - Structure Correlations

Crystalline metals showing structure in the resistivity (i.e.,resistivity minima and, or maxima) usually have a more pronounced structure in the thermoelectric power (see 9,10).

For the set of samples studied in this work it can be seen that Metglas 2605A has resistivity structure (two minima and a maximum)and nearly linear thermoelectric power. Metglas 2826 may have some thermoelectric power structure and a minimum in resistivity around 20K. Metglas 2204 is consistent in not showing structure in both resistivity and thermoelectric power within the experimental temperature range.

All samples considered it seems impossible to make any correlations bewteen the nature of the resistivity and the results obtained for the thermoelectric power on the basis of any of the existing theories.

IV - 5 - Effect of the Composition of the Alloy

Studying the magnitude of the thermoelectric power experimentally obtained one sees that Metglas 2826A has an extremely small thermoelectric power, small even when compared to Metglas 2826.

Such difference in magnitude between these two samples might arise from the addition of Cr or to the additional 2% transition metal in the Metglas 2826A alloy, deviating from the usual 80 % transition metal - 20% glass former, as in Metglas 2826.

This question could not be answered definitely with the set of samples svailable to us at the moment, but the suggestion made by Cochrane et al.[19] and Levy and Rayne,[20] that the elements Cr and Mo produce a resonance like contribution to the high temperature resistivity, favors the view that indeed it is the presence of Cr that induces the change in magnitude of the thermoelectric power between the two samples.

In fact, if one compares Metglas 2605 to Metglas 2605A, which differ by a 2% Mo content (keeping the 80% transition metal-20% glass former composition) it can be seen that the substitution of iron by Mo induces a reduction in the magnitude of the thermoelectric power by a factor around 2.

Figure 11

The solid lines represent the average of the results obtained by three independent groups.

The dotted line reproduces the data published by Nagel.[4]

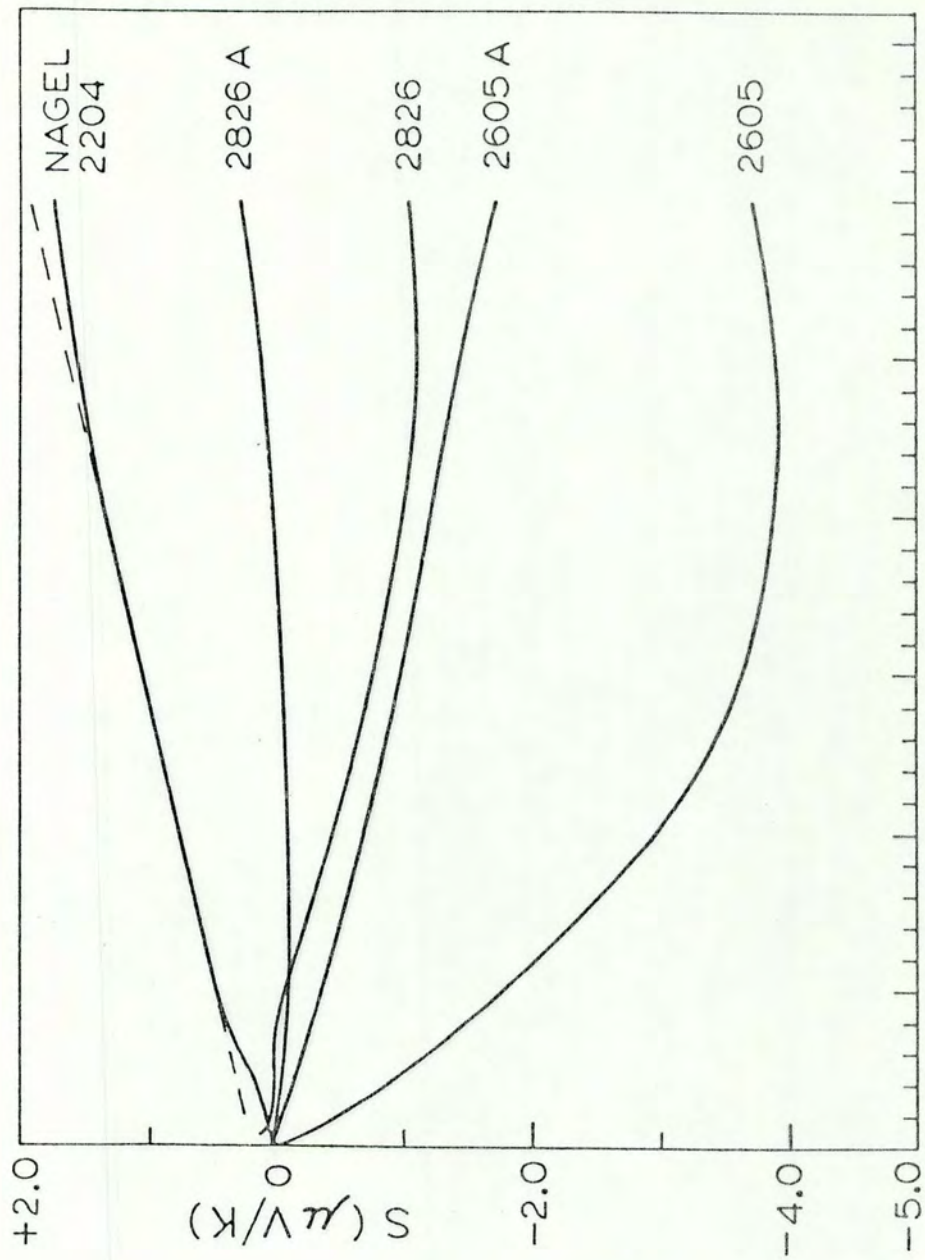
NAGEL
2204
2826 A
2826
2605 A
2605
+2.0
0
-2.0
-4.0
-5.0
S (μV/K)
0
100
200
300
T(K)

IV - 6 -General Considerations

Analyzing the experimental results obtained and the predictions of the several theories proposed we are led to say that not one individual theory can explain all of the features presented.

In order to assess the physical consistency of this assumption, further studies of thermoelectric powers of metallic glasses should be undertaken.

V - CONCLUSIONS

The study of thermoelectric power of some amorphous metallic alloys proved to be of limited use in the understanding of the processes involved in electronic transport phenomena in metallic glasses.

The Ziman theory seems to explain the results for only one of the samples (Metglas 2204) over a limited temperature interval (40 to 250K). Our results agree remarkably well with the curve found by Nagel[4] over the temperature range quoted above. Metglas 2204 is the only non ferromagnetic material in the set of five samples measured.

The reappearance of a straight line in Metglas 2204 below 15K cannot be attributed to the same process as the high temperature results since the thermoelectric power as a function of temperature has a different slope in the two regions.

The existence of a Kondo or Kondo-like process contributing to the thermoelectric power of amorphous metals is still in doubt since these processes contribute to the thermoelectric power through the Nordheim-Görter rule. This rule says that the total thermopower of a metal is the result of the resistance weighted average of each of the processes involved. Thus the Kondo-type contribution to the thermoelectric power will be reduced by a factor 10^{-3} to 10^{-2} (which represents the ratio $\rho_{\text{Kondo-like}}/\rho_{\text{total}}$). The thermoelectric power of amorphous

metals will be sensitive only to the mechanism that produces the predominant scattering because of the weight of the total resistivity in metallic glasses. This made it difficult if not impossible to detect the Kondo-type contribution to the thermoelectric power with the experimental resolution available to us.

The presence of Cr or Mo in the composition of a metallic glass appears to be connected with a reduction in the magnitude of the thermoelectric power apparently due to the introduction of localized and possibly resonant scattering centres in amorphous alloys.

This set of measurements hardly represents a complete study of the thermoelectric power of amorphous metals, but it is sufficient to show the diversity of behaviour, enabling us to make the following suggestions:

a) To better understand the behaviour of metallic glasses, the thermoelectric power for recrystallized samples should be measured and compared to the amorphous results.

b) The thermoelectric powers of a series of amorphous alloys with the same components but with varied proportions should also be measured.

These procedures should reveal the influence of the structure or the composition on the thermoelectric power of metallic glasses.

BIBLIOGRAPHY

1) R.W. Cochrane, Journal de Physique, Colloque C6, supp. au no 8, 39 (1978).

2) J.J. Gilman, Phys. Today, May 1975, pp 46-53.

3) A few of the names most commonly associated with this field are: C.C. Tsuei (IBM); R. Hasegawa (Allied Chemical Corp.); R.A. Levy (RPI); S.R. Nagel (University of Chicago); R.W. Cochrane (Université de Montréal); J. Strom-Olsen, R. Harris and M.J. Zuckermann (McGill University); and H.J. Güntherodt (University of Basel, Switzerland).

4) S.R. Nagel, Phys. Rev. Letters 41, 990 (1978).

5) Metglas is a proprietory name for amorphous metallic materials available from Allied Chemical Company, Morristown, N.Y. 07960 USA.

6) G. Borelius, W.H. Keesom, C.H. Johansson, Proc. Acad. Sci. Amst. 31, 1046 (1928).

G. Borelius, W.H. Keesom, C.H. Johansson and J.O. Linde, Proc. Acad. Sci.Amst. 33, 17 (1930).

G. Borelius,W.H. Keesom, C.H. Johansson and J.O. Linde, Proc. Acad. Sci. Amst. 34, 1365 (1931).

G. Borelius,W.H. Keesom, C.H. Johansson and J.O. Linde, Proc. Acad. Sci. Amst. 35, 10 (1932).

7) R.B. Roberts, Phil. Mag. 36, 91 (1977).

8) Thermoelectricity: An introduction to the principles, D.K.C. MacDonald, John Wiley & Sons, Inc. , New York, London (1962).

9) Thermoelectricity in Metals and Alloys, R.D. Barnard, Taylor and Francis Ltd., London (1972).

10) Thermoelectric Power of Metals, F.J. Blatt, P.A. Schroeder, C.L. Foiles and D. Greig, Plenum Press, New York, London (1976).

11) S.R. Nagel and J. Tauc, Phys. Rev. Letters 35, 380 (1975).

12) C.C. Tsuei and R. Hasegawa, Solid State Comm. 7, 1581 (1969).

13) R.W. Cochrane, R. Harris, J.O. Strøm-Olsen and M.J. Zuckermann, Phys. Rev. Letters 35, 676 (1975).

14) J. Kondo: Solid State Physics 23, 184 (1969).

15) R. Asomoza and A. Laborde, private communication.

16) G.S. Grest and S.R. Nagel, to be published.

17) M.N. Baibich and W.B. Muir, unpublished data.

18) J.A. Rayne and R.A. Levy, in Amorphous Magnetism II,319 (ed. Levy & Hasegawa) (1977).

19) R.W. Cochrane, F.T. Hedgcock, B.J. Kästner and W.B. Muir, Journal de Physique, Colloque C6, supp. au no 8, 39, C6-939 (1978).

20) R. Levy and J. Rayne , in Amorphous Magnetism II, (ed. Levy & Hasegawa) (1977); Bull. Am. Phys. Soc. 23, 413 (1978).